A Study of Non-sequential Double Ionization of Atoms in Circularly Polarized Laser Fields Using Classical-trajectory Simulations

Research Thesis

Presented in partial fulfillment of the requirements for graduation
with research distinction in Physics in the undergraduate
colleges of The Ohio State University

by
Xiaowei Gong

The Ohio State University
April 2017

Project Advisor: Professor Louis DiMauro, Department of Physics

Abstract

The development of ultrashort pulse laser technologies has enabled the studies of ionization of atoms and molecules in intense laser fields (with intensity on the order of 10^{14} $\mathrm{W/cm^2}$ or higher) over the last three decades. Many novel physical phenomena have been discovered, including non-sequential double ionization. This process results in a drastic enhancement in the yield of doubly charged ion in measurements of ionization yields of atoms subjected to intense field. Its mechanism can be explained using the semi-classical model of strong field ionization. First, an electron of the atom is ionized by the strong laser field. Then the electron is accelerated by the laser field and recollides with the parent ion and knocks out another electron. This process should be suppressed when the laser field is circularly polarized because recollision is impossible in this case. It is consistent with early experimental results. However, the observation of enhancement in doubly charged ion yield in a later experiment on magnesium atoms seems to contradict with the previous explanation. Further theoretical studies suggested that recollision is in fact possible under certain conditions. However, so far most of the theoretical and experimental studies on this problem have been only focused on the case of magnesium atom at laser wavelength of 800nm.

In this thesis, we present a theoretical study of non-sequential double ionization for the case of circularly polarized fields using two-electron classical-trajectory Monte-Carlo simulations at various laser wavelength and ionization potentials. We study the contributions of sequential and non-sequential ionization processes as a function of laser intensity. We also investigate the characteristics of recolliding trajectories.

List of Figures

List of Tables

Table of Contents

1. Introduction

Non-sequential double ionization has been an important topic in strong field atomic physics. Early studies of non-sequential double ionization focused on the case of linearly polarized laser field [1,2] in which an electron is first ionized from the atom and then driven by the laser field to recollide with the parent ion and knock out another electron. It was commonly believed that this process should be suppressed in circularly polarized field since a free electron in a circularly polarized field tends to spiral away from the origin so recollisions are unlikely to happen. This theory is supported by the experimental results of noble gases atoms. However, later experimental observations of non-sequential double ionization under circularly polarized light in Mg [3] and varies of diatomic molecules like NO and O_2 [4] seem to contradict the results of noble gases.

The conflicting evidence between different targets has motivated theoretical efforts. Mauger et al [5] presented two-electron classical trajectory simulations to explain how recollisions become significant under circularly polarized field due to the influence of electron-electron and electron-ion core interaction under certain conditions. Fu et al [6] have proposed laser wavelength and ionization potential criteria for observing non-sequential double ionization in circularly polarized field. They suggested that alkali-earth atoms are suitable candidates for abnormal non-sequential double ionization study due to their low ionization potentials.

To shed more light on the problem, we conduct a systematic theoretical investigation on atoms Mg, Ca, Zn and Xe which have low ionization potentials. This thesis is devoted to a theoretical study on non-sequential double ionization using two-electron classical trajectory

simulations.

The dynamics of photoelectron in strong field ionization can be modeled using a semiclassical model [8,9] in which an electron first tunnel ionizes and the subsequent motion is treated as a free particle in the laser field. In linear polarization, after the electron is ionized, the motion of the electron is driven by the laser field which is a sinusoidal wave. Classically, the motion of the electron can be analyzed by solving the second order differential equation

$$\mathrm{m}\frac{d^2x}{dt^2} = \ -\mathrm{eF}_0 cos(\omega t). \tag{1}$$

After solving the differential equation, we obtain

$$\mathrm{x(t)} = \ \frac{\mathrm{F}_0}{m\omega^2}[\cos(\omega t) - \cos(\omega t') + \sin(\omega t')\omega_0(t - t')], \tag{2}$$

where F_0 is the amplitude of electric field.

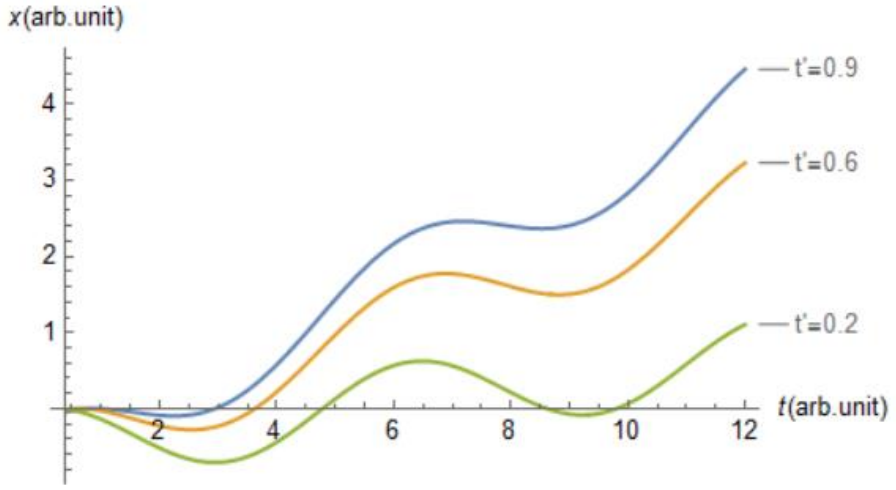

Figure 1: The position of first electron. The electron will come back to recollide to the ion.

Depending on the instant of ionization t', the electron may or may not come back to the origin. Figure 1 shows the position of the electron as a function of time for different values of t'. As shown in Figure 1, when $t' > 0$, the curves will across the x-axis again, which means that the double ionization occurs.

Over the last two decades, there has been a lot of study on ionizations in strong field, including the double ionization. The experimental data of single and double ionization yields

of Helium with linearly polarized 100fs, 780nm laser pulses as functions of the intensity is shown in Figure 2. The points are experimental data and the solid curves are quantum mechanical simulations assuming sequential ionization. In the intensity range between $2\times10^{14}W/cm^2$ to $5\times10^{15}W/cm^2$, the sequential ionization theory does not match the data because the yield is a lot higher than expected. The sequential ionization theory matches the data in the intensity range between $5\times10^{15}W/cm^2$ to $10^{16}W/cm^2$. As intensity goes really high, although recollision process can still happen, the probability of sequential ionization starts to dominate. Thus, the data matches with the sequential ionization theory. Non-sequential ionizations of noble gases atoms were shown to be absence in the case of circular polarization, which supported the origin of the process was due to rescattering. The observed enhancement feature in the doubly charged ion yields is called the "knee" structure.

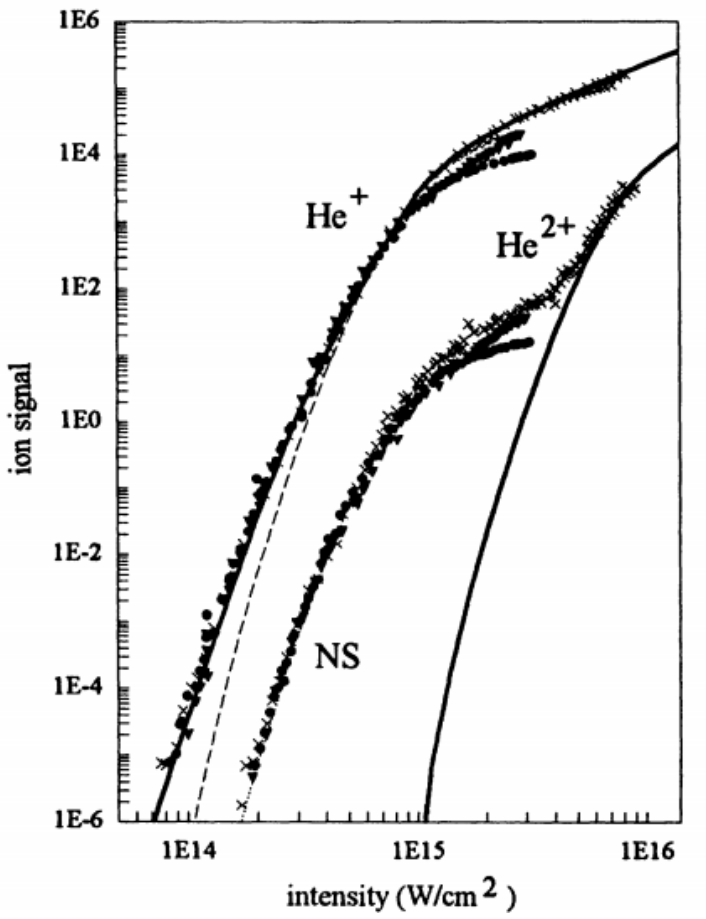

Figure 2: Single and double ionization of Helium in intense near infrared laser field From [1].

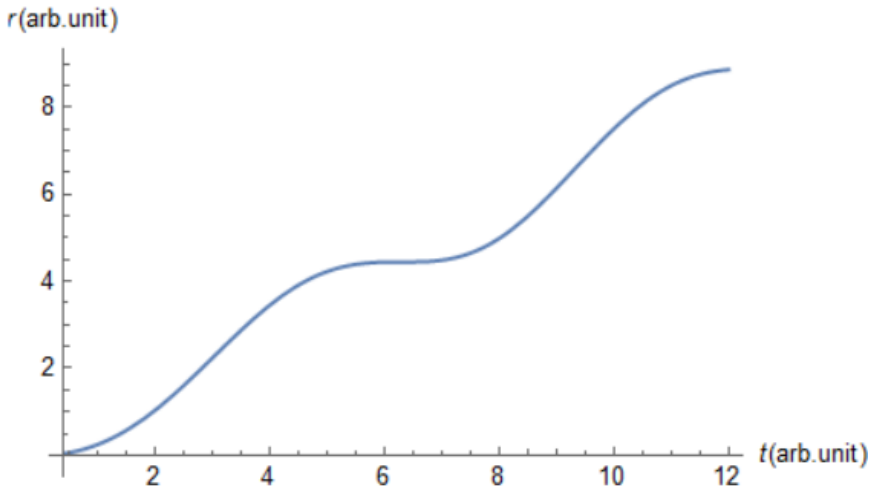

Figure 3: Motion of an electron in circularly polarized field.

As mentioned before, recollisions happen due to the laser field in linear polarization. However, this is not the case for circular polarization. Without Coulomb potential, the equation of motion is for the case of circular polarization is

$$\mathrm{m}\frac{d^2\vec{r}}{dt^2} = -\mathrm{e}\frac{F_0}{\sqrt{2}}[cos(\omega_0 t)\hat{x} + \sin(\omega_0 t)\hat{y}]. \quad (3)$$

After solving the differential equation, we obtain

$$\mathrm{x(t)} = \frac{eF_0}{\sqrt{2}m\omega^2}[\cos(\omega_0 t) - \cos(\omega_0 t') + \sin(\omega_0 t')\omega_0(t-t') \quad (4)$$

$$\mathrm{y(t)} = \frac{eF_0}{\sqrt{2}m\omega^2}[\sin(\omega_0 t) - \sin(\omega_0 t') - \cos(\omega_0 t')\omega_0(t-t'). \quad (5)$$

As shown in Figure 3, in circular polarization, the electron would not come back to recollide with the ion, where $\mathrm{r} = \sqrt{x^2 + y^2}$ is the position of the electron. Figure 4 shows a plot of the electron position in x and y coordinates. As shown, the trajectory spirals away from the ion so the rescattering cannot happen.

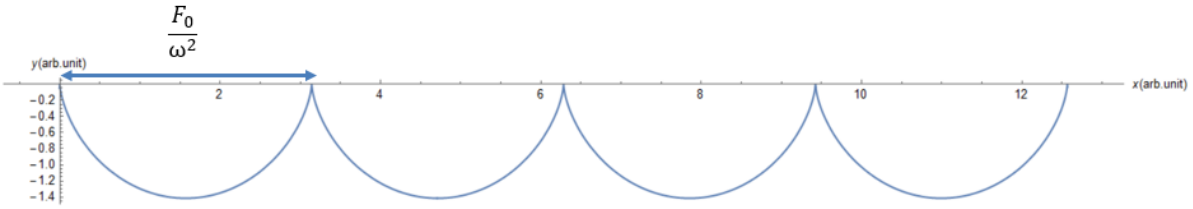

Figure 4: The motion of electron in circularly polarized field in xy plane. $\frac{\mathrm{F_0}}{\omega^2}$ is called the quiver amplitude.

Indeed, it was shown in experiments on noble gas atoms that “knee” structure was absent in circularly polarized fields. However, a later experiment on Mg atoms [3] seems to bring an unexpected result. Figure 5 is the experimental ion yields as a function of laser intensity of Mg atoms irradiated by 800nm, circularly polarized. The black dots are single ionization yields and the circles are double ionization yields. Surprisingly, a “knee” structure appears in the doubly charged ion yield curve. It is not clear whether this feature has the same origin as in the one shown in Figure 2.

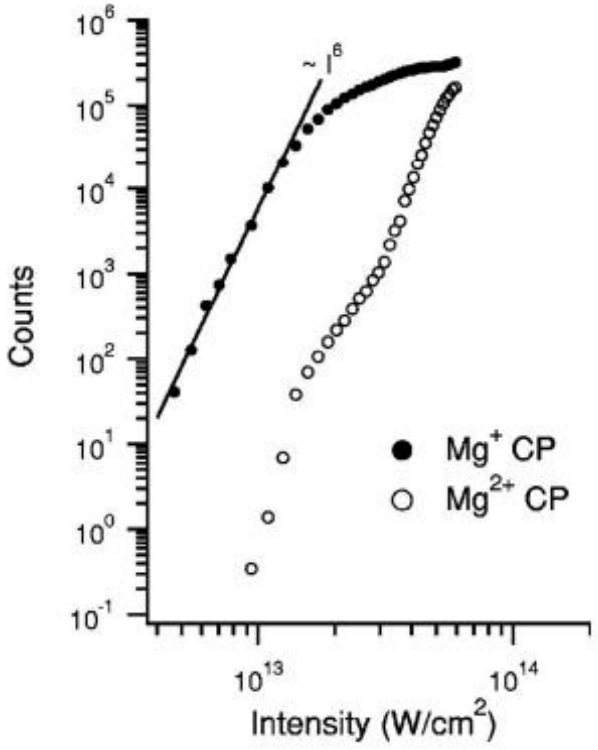

Figure 5: Single and double ionization of Magnesium in intense near infrared laser field. From [3].

A later theoretical study [5] provided an explanation for the “knee” structure in the Mg results. The theoretical calculations of Mg and He in circular polarization from Ref. [5] are shown in Figure 6. The probability of non-sequential double ionization is high for Mg. However, for He, the “knee” structure disappear. The reason is that the ionization potential (I_p) of He is bigger than Mg. Further discussions will be presented in section 4.

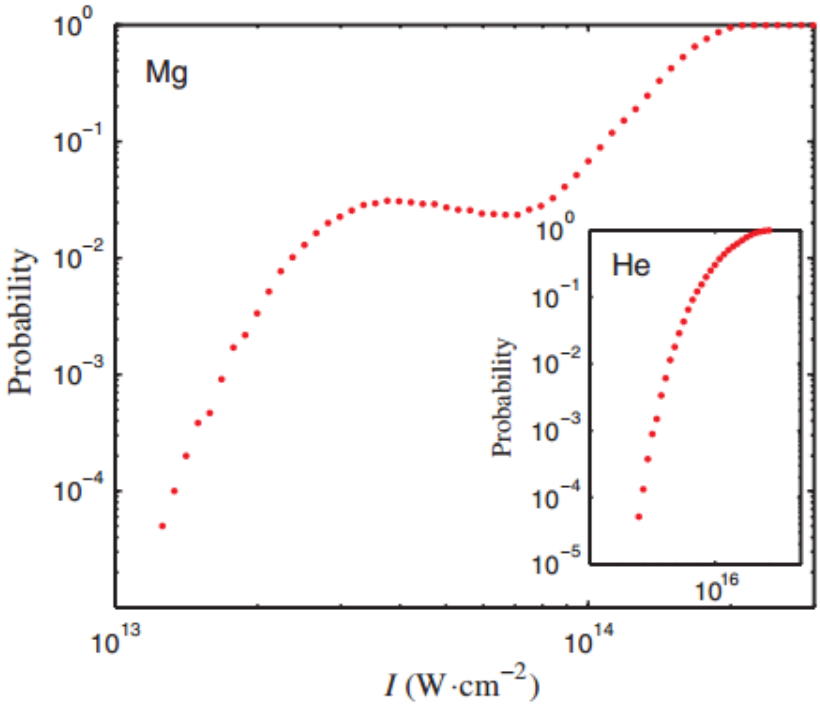

Figure 6: Double ionization of Magnesium and Helium in intense near infrared laser field. From [5].

2. Theory

Our theoretical simulations follow the method presented in [5,7]. In order to study the double ionization, we start with a classical model of a two-electron atomic system in a laser field. The Hamiltonian is written as

$$H = \frac{1}{2}mv_1^2 + \frac{1}{2}mv_2^2 - \frac{2}{\sqrt{r_1^2+a^2}} - \frac{2}{\sqrt{r_2^2+a^2}} + \frac{1}{\sqrt{r_{12}^2+b^2}} - \vec{F}(t)\cdot\vec{r_1} - \vec{F}(t)\cdot\vec{r_2} \quad . \quad , \quad (6)$$

where v_1 and v_2 are the velocities of the two electrons respectively, $r_{12} = \sqrt{(x_1-x_2)^2+(y_1-y_2)^2+(z_1-z_2)^2}$, $r_1 = \sqrt{x_1^2+y_1^2+z_1^2}$ and $r_2 = \sqrt{x_2^2+y_2^2+z_2^2}$. r_{12} is the distance between the two electrons. r_1 is the distance between electron 1 and ion. r_2 is the distance between electron 2 and ion. Unless specified otherwise, atomic unit is used in this thesis (e=1, m=1, $\frac{1}{4\pi\varepsilon_0} = 1$). The first and second terms are Coulomb interaction between the two electrons and the ion respectively. The ion is assumed to remain stationary at the origin of the coordinate system. The third term is coulomb interaction between the two electrons. The last two terms are due to the laser field.

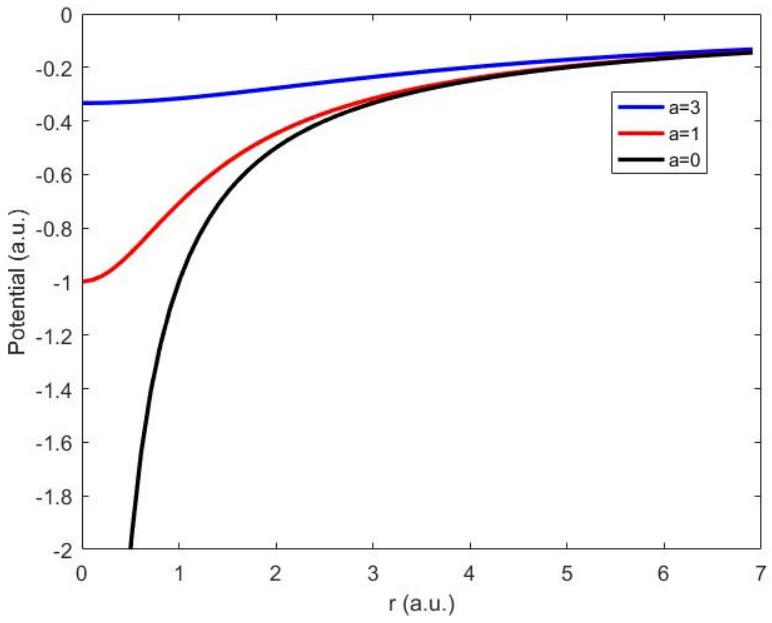

Figure 7: Ionization potential with different value of *a*.

There are two soft core parameters *a* and *b*. *a* is used to avoid singularity in calculations and mimic the ionization potential of the system. As shown in Figure 7, when *a* is large, it is a weakly bounded system which has low ionization potential energy. When *a* is small, it is a strongly bounded system. *b* is used to reduce the repulsive force between electrons; otherwise autoionizations may occur.

The electric field profile of a laser pulse $F(\mathrm{t})$ can be written as

$$F(t) = F_0(\mathrm{t})\cos(\omega t), \tag{7}$$

where $F_0(\mathrm{t})$ is the envelope of the pulse and ω is the frequency of the carrier wave. In our simulations, we use sine-squared envelope, that is,

$$F(t) = F_0 sin^2(\frac{2\omega t}{11n})\cos(\omega t), \tag{8}$$

where F_0 is the peak field amplitude and n is the full with of half maximum (FWHM) pulse duration in terms of number of optical cycles of the intensity profile. Figure 8 shows a laser pulse with five optical cycles long at FWHM. For circular polarization, the pulse is expressed as

$$F(t) = \frac{F_0}{\sqrt{2}} sin^2\left(\frac{2\omega t}{11n}\right)[\cos(\omega t)\,\hat{x} + \cos(\omega t)\,\hat{y}], \tag{9}$$

All the simulations in the thesis are performed with this pulse.

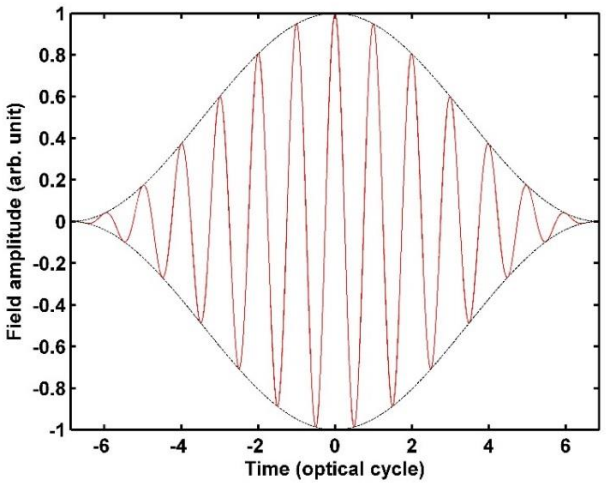

Figure 8: Laser pulse with five optical cycles long at FWHM.

In this classical model, the initial states of the electrons are mimicked by random distributions of initial positions and velocities. The total energy, E, of the system is equal to the sum of ionization energies of the atom and the singly charged ion of the atom

$$E = KE + PE. \tag{10}$$

The kinetic energy (KE) is

$$KE = \frac{1}{2}\, m\, {v_1}^2 + \frac{1}{2}\, m\, {v_2}^2, \tag{11}$$

where $v_1 = \sqrt{{v_{1x}}^2 + {v_{1y}}^2 + {v_{1z}}^2}$ and $v_2 = \sqrt{{v_{2x}}^2 + {v_{2y}}^2 + {v_{2z}}^2}$.

The potential energy (PE) is

$$PE = -\frac{2}{\sqrt{{r_1}^2+a^2}} - \frac{2}{\sqrt{{r_2}^2+a^2}} + \frac{1}{\sqrt{{r_{12}}^2+b^2}}. \tag{12}$$

The equations of motions for the two electrons are

$$m\frac{d^2\overrightarrow{r_1}}{dt^2} = -\nabla\left(-\frac{2}{\sqrt{{r_1}^2+a^2}} + \frac{1}{\sqrt{{r_{12}}^2+b^2}}\right) - \overrightarrow{F_x}(t) \tag{13}$$

$$m\frac{d^2\overrightarrow{r_2}}{dt^2} = -\nabla\left(-\frac{2}{\sqrt{{r_2}^2+a^2}} + \frac{1}{\sqrt{{r_{12}}^2+b^2}}\right) - \overrightarrow{F_y}(t). \tag{14}$$

Different initial conditions of two electrons can have different trajectories. At the end, if $KE \geq 0$, the electron can be ionized. If KE<0, the electron cannot be ionized.

3. Simulations Procedures

3.1 Generation of Initial Conditions

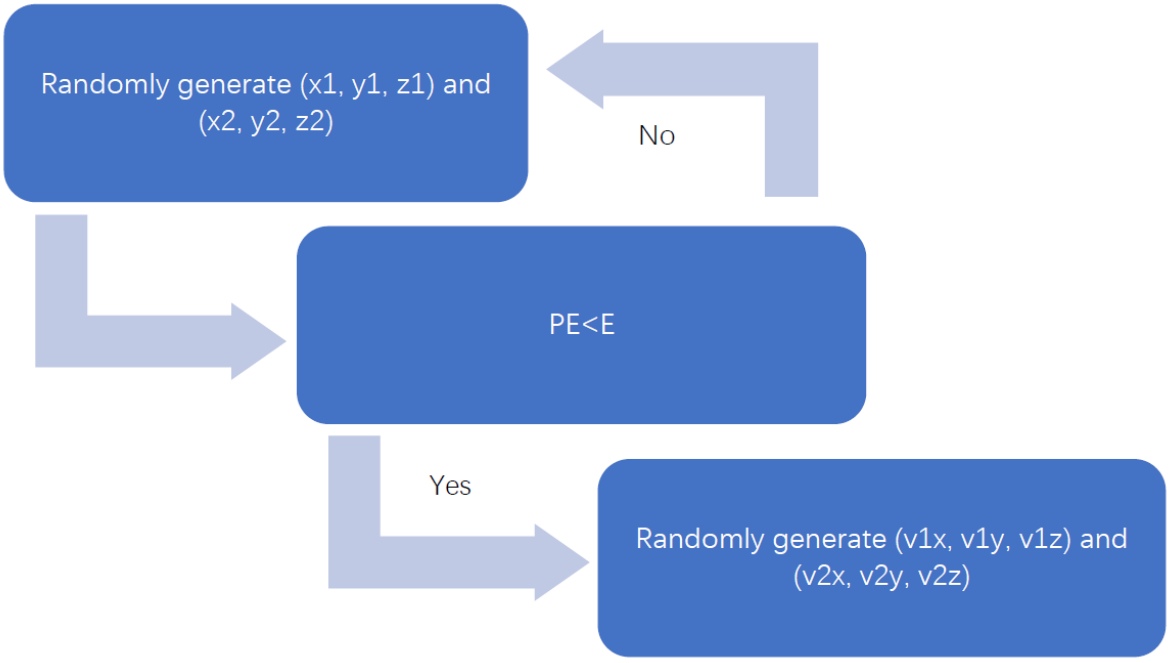

Figure 9: Procedures of determine the initial conditions.

Our simulations are performed by using MATLAB. The first step is to set the distributions of the initial positions and velocities of the two electrons. As described in Figure 9, we first generate a set of initial positions of two electrons $(x_1,\ y_1,\ z_1,\ x_2,\ y_2,\ z_2)$ randomly. Then we calculate the sum of potential energies of the two electrons (PE). Since the kinetic energy should always be positive, PE has to be less than E. If this constraint is satisfied, we calculate the sum of kinetic energies KE of the two electrons which is given by

$$\mathrm{KE} = \mathrm{E} - \mathrm{PE}. \tag{15}$$

If not, we generate the initial positions again.

After calculating KE, the values of velocity components of each electron should distribute randomly. In order to do that, we split KE is randomly into two parts, KE1 and KE2, for the two electrons, where

$$KE_1 = \frac{1}{2}\, m(\, {v_{1x}}^2 + {v_{1y}}^2 + {v_{1z}}^2) \tag{16}$$

$$KE_2 = \frac{1}{2}\, m(\, {v_{2x}}^2 + {v_{2y}}^2 + {v_{2z}}^2). \tag{17}$$

After rearranging them, we get

$${v_{1x}}^2 + {v_{1y}}^2 + {v_{1z}}^2 = \frac{2}{m} KE_1 \tag{18}$$

$${v_{2x}}^2 + {v_{2y}}^2 + {v_{2z}}^2 = \frac{2}{m} KE_2, \tag{19}$$

which are the equations of sphere. Therefore, getting random distributions for the velocity components is equivalent to picking random points on a spherical surface. The procedures in figure 9 are repeated until sufficient numbers (~10^5) of valid sets of initial conditions are generated.

The correlation of the positions of electron 1 and electron 2 is shown in Figure 10. The shape shows that the two electrons tend to separate because the Coulomb force between two electrons repels with each other. For the Figure 10 (b), when the velocity of first electron gets bigger, the velocity of second electron gets smaller. The reason is that since the total kinetic energy is equal to the addition of two kinetic energies of electrons, when KE1 gets bigger, KE2 becomes smaller.

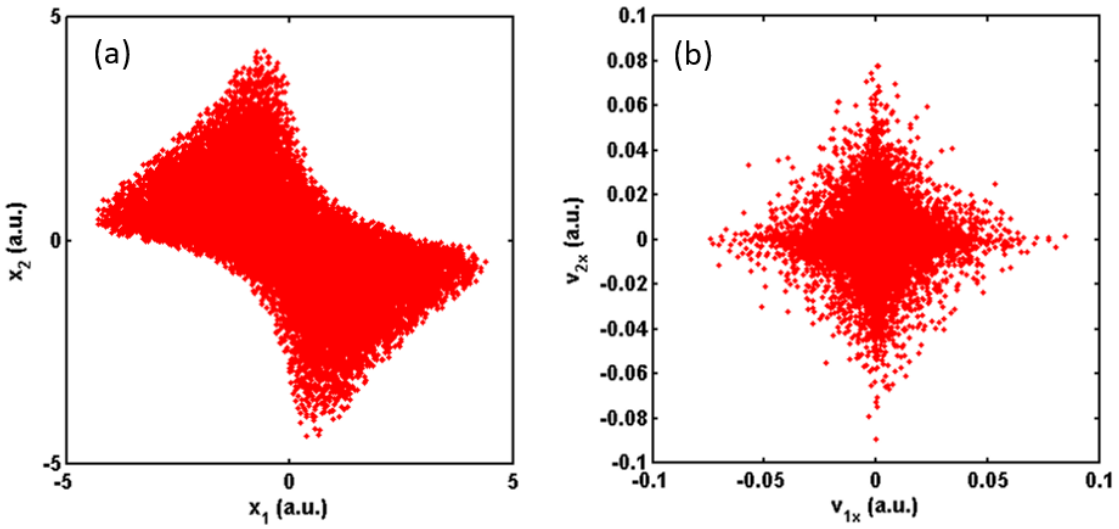

Figure 10: The correlation between the initial conditions of electron 1 and electron 2 of Magnesium. a) The correlation of position. b) The correlation of velocity.

However, there are some restrictions to generate the initial positions. Certainly, it is not practical to generate the random initial positions between 0 to infinity. In fact, the position of electron cannot be too far away from ion because the PE would be too large. It would be useful to have a rough estimate on the largest possible distance between the electron and the ion x_{max}. To do that, we consider the potential energies in the configurations of electrons shown in Figure 11. For simplicity, the potential energy due to electron-electron interaction is ignored. For case a,

$$-\frac{4}{\sqrt{{x_{max}}^2+a^2}} = E. \tag{20}$$

For case b,

$$-\frac{2}{\sqrt{{x_{max}}^2+a^2}} - \frac{2}{\sqrt{a^2}} = E. \tag{21}$$

Since we ignore the electron-electron Coulomb potential, $PE_a = PE_c$. By comparing three cases, we observe case b has the biggest $x_{\max}$. After solving the inequation and plugging the different a value for different atom in

$$x_{max} = \sqrt{\frac{4}{(E+\frac{2}{a})^2} - a^2}, \tag{22}$$

we can get different values of x_{max} for different atoms.

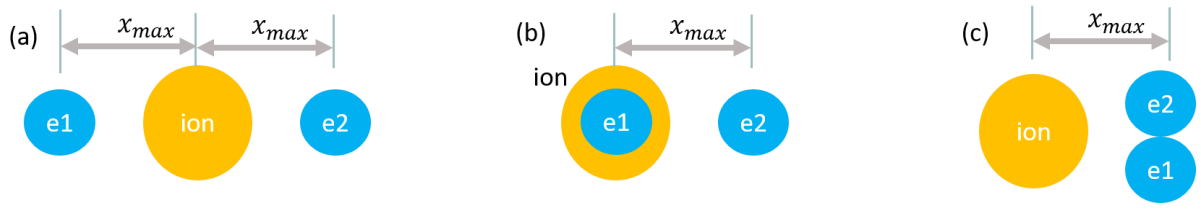

Figure 11: Different initial positions of electron 1 and electron 2.

3.2 Determination of a Values for Different Atoms

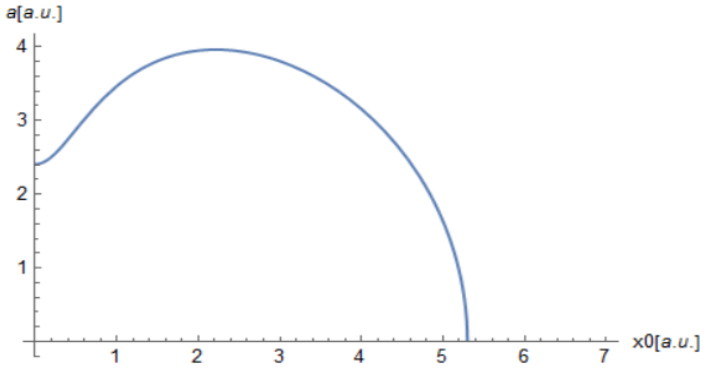

Figure 12: The upper limit of a as a function of as x_0 for Calcium atom.

As mentioned in the section 2, the value of soft core parameter a has a certain range which depends on the ionization potential of the atom. When a becomes larger, PE becomes larger because PE<0. If a is very large, we may have PE>E. In order to get the largest possible a, we want to find the largest PE in which PE<E in at least one case in Figure 11. If it exceeds the largest possible value, the Equation (10) cannot be satisfied. Considering different situation of initial conditions, we claim that PE_a is the smallest one. For case a in Figure 11, we get

$$PE_a = -\frac{4}{\sqrt{{x_0}^2+a^2}} + \frac{1}{\sqrt{(2x_0)^2+b^2}} \leq E. \tag{23}$$

After solving the inequality, we get

$$a^2 \leq \left(\frac{4}{-E+\frac{1}{\sqrt{4{x_0}^2+b^2}}}\right)^2 - {x_0}^2. \tag{24}$$

Using inequality (24), one can find an upper limit of a. Figure 12 shows the upper limit of a for Ca atom. On the other hand, when a is too small, the electrons can be ionized without laser field. The values of a that we use for different atom is shown in Table 1.

	Range of a	a
Ca	3.1 – 3.9	3.7
Mg	2.6 – 3.2	3
Zn	2 – 2.6	2.4
Xe	1.8 – 2.2	2

Table 1: Value of a for different atoms.

3.3 Solving Equations of Motion

After setting the initial conditions, we solve the equations of motion. We have 6 second order differential equation, 3 for each electron. In order to use MATLAB Runge-Kutta algorithm to solve the equations, we decompose them to 12 first order differential equations. The electron is ionized when energy is greater than 0. The position is $(x_1,\ y_1,\ z_1)$ for electron 1 and $(x_2,\ y_2,\ z_2)$ for electron 2.

$$\frac{dx_1}{dt} = v_{1x}$$

$$\frac{dv_{1x}}{dt} = -\frac{2x_1}{\left({x_1}^2 + {y_1}^2 + {z_1}^2 + a^2\right)^{3/2}} + \frac{(x_1 - x_2)}{\left[(x_1 - x_2)^2 + (y_1 - y_2)^2 + (z_1 - z_2)^2 + b^2\right]^{3/2}} - F_x(t)$$

$$\frac{dx_2}{dt} = v_{2x}$$

$$\frac{dv_{2x}}{dt} = -\frac{2x_2}{\left({x_2}^2 + {y_2}^2 + {z_2}^2 + a^2\right)^{3/2}} + \frac{(x_2 - x_1)}{\left[(x_1 - x_2)^2 + (y_1 - y_2)^2 + (z_1 - z_2)^2 + b^2\right]^{3/2}} - F_x(t)$$

$$\frac{dy_1}{dt} = v_{1y}$$

$$\frac{dv_{1y}}{dt} = -\frac{2y_1}{\left({x_1}^2 + {y_1}^2 + {z_1}^2 + a^2\right)^{3/2}} + \frac{(y_1 - y_2)}{\left[(x_1 - x_2)^2 + (y_1 - y_2)^2 + (z_1 - z_2)^2 + b^2\right]^{3/2}} - F_y(t)$$

$$\frac{dy_2}{dt} = v_{2y}$$

$$\frac{dv_{2y}}{dt} = -\frac{2y_2}{\left({x_1}^2 + {y_1}^2 + {z_1}^2 + a^2\right)^{3/2}} + \frac{(y_2 - y_1)}{\left[(x_1 - x_2)^2 + (y_1 - y_2)^2 + (z_1 - z_2)^2 + b^2\right]^{3/2}} - F_y(t)$$

$$\frac{dz_1}{dt} = v_{1z}$$

$$\frac{dv_{1z}}{dt} = -\frac{2z_1}{\left({x_1}^2 + {y_1}^2 + {z_1}^2 + a^2\right)^{3/2}} + \frac{(z_1 - z_2)}{\left[(x_1 - x_2)^2 + (y_1 - y_2)^2 + (z_1 - z_2)^2 + b^2\right]^{3/2}}$$

$$\frac{dz_2}{dt} = v_{2z}$$

$$\frac{dv_{2z}}{dt} = -\frac{2z_2}{\left({x_1}^2 + {y_1}^2 + {z_1}^2 + a^2\right)^{3/2}} + \frac{(z_2 - z_1)}{\left[(x_1 - x_2)^2 + (y_1 - y_2)^2 + (z_1 - z_2)^2 + b^2\right]^{3/2}}$$

(25-36)

4. Results and Discussions

4.1 Wavelength and Target Dependence

Previously, as shown in Figure 4, the quiver amplitude depends on the field strength and the wavelength of the laser. Figure 13 (a) shows the double ionization data of Mg, (b) is for Zn and (c) is for Xe. Mg has the most pronounced "knee" structure that the probability is 2×10^{-2}. The enhancement in Zn is much weaker which is 10^{-3} and Xe does not have this feature at all. The reason is that Mg has the smallest I_p and Xe has the largest I_p. As I_p gets higher, larger field strength is required to ionize the first electron, which means the quiver amplitude is large. Thus, it is more difficult to have the recollision.

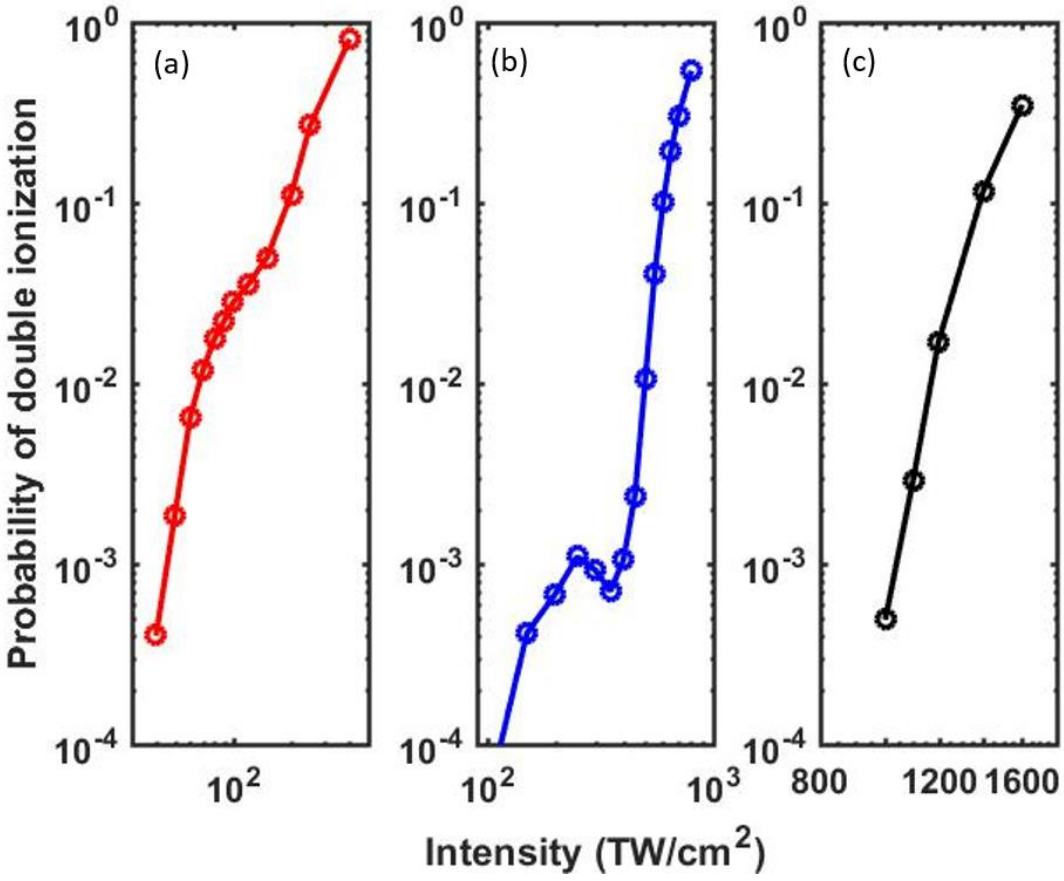

Figure 13: Simulated yields of double ionization for different atoms. (a) Double ionization data for Magnesium. (b) Double ionization data for Zinc. c) Double ionization data for Xenon.

Similarly, the shorter wavelength results in higher double ionization probability. Figure 14 shows the double ionization probability of different atoms with different laser wavelengths.

For the same atom, the probability is higher when the wavelength is shorter. The reason is that shorter wavelength results in smaller quiver amplitude, so the electron is more likely to go back and recollide with the ion.

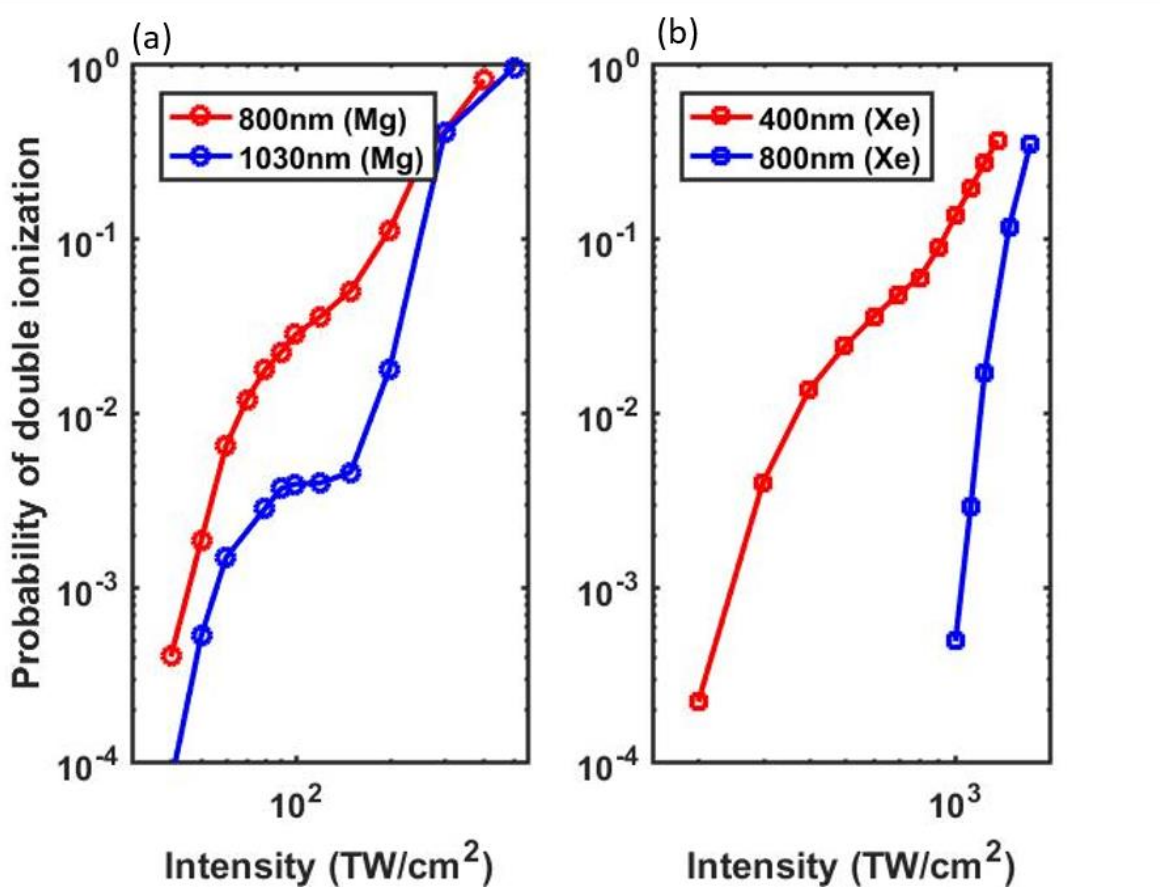

Figure 14: Simulated single and double ionization yields with different wavelength. a) Double ionization data for Magnesium. b) Double ionization data for Xenon.

4.2 Distinguishing Sequential and Non-sequential Process

After doing the calculation, we analysis the results of Xe with 400nm laser circular polarization. There are two different processes for double ionization: sequential and non-sequential. Sequential double ionization is that the first electron is ionized followed by the second electron is ionized. For atoms in intense infrared laser fields, after the first electron is ionized, it can go back towards the ion. If the returning electron has enough energy, another electron will be knocked out and is ionized together with the first electron, which is the non-sequential double ionization.

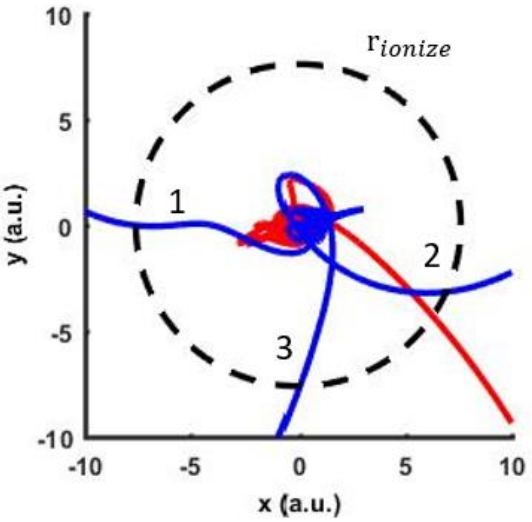

Figure 15: Electrons trajectories of a double ionization event. When the distance between an electron and the ion is greater than r_{ionize} , it is considered to be ionized. The number of the blue curve is the order that the first ionized electron pass through the boundary.

In order to distinguish the two processes in the simulations, we analyze individual electron trajectories. As shown in Figure 15, a spherical boundary which radius is $r_0 = 5 < \sqrt{x^2 + y^2 + z^2} >$ is set up to study the ionization. Whenever an electron passes outside this boundary, it is considered to be ionized. If the electron can pass through the boundary and return at a later time, recollision might happen. In the simulations, we record the time values whenever the trajectory exit or re-enter the spherical region. An electron may pass through the boundary multiple times, the last time that it goes out is determined to be the ionization time.

Figure 16 shows the correlation between t_1 and t_2, where t_1 is the ionization time of electron 1 and t_2 is the ionization time for the electron 2. Panel (a) shows the result at an intensity of $400\ \mathrm{TW/cm^2}$ and panel (b) shows the result at an intensity of $800\ \mathrm{TW/cm^2}$. The behaviors of non-sequential double ionization and sequential double ionization are different at low intensity and high intensity. At low intensity, the distribution is close to $t_1 = t_2$, which suggests that the domination is non-sequential double ionization. Since the intensity is low, it is not easy for the laser field to drive the second electron to "escape" from the ion. If the first electron can come back to collide the second electron, it is more likely to have double ionization. As shown in (b), at high intensity, two more "islands" appear on the side, either t_1 is significantly earlier than t_2 or vice versa. These are sequential ionization events.

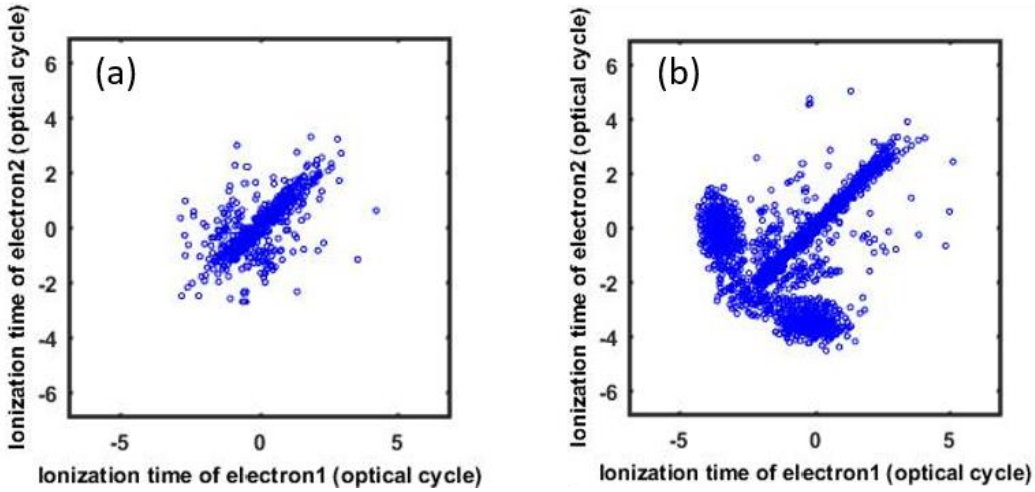

Figure 16: Correlation of ionization time between electron 1 and electron 2 of Xenon. a) The result of intensity of $400\ \mathrm{TW/cm^2}$ b) The result of intensity of $800\ \mathrm{TW/cm^2}$.

On the contrary, if we exclude the electron-electron repulsion term in the simulations, the ionization time of the two electrons will be uncorrelated. Figure 17 shows that the distribution can be everywhere without the Coulomb interaction of two electrons. When they have Coulomb interaction, after the first electron is ionized, the second electron is attracted to the ion, which makes the second electron ionized harder. If the Coulomb interaction disappears, the two electrons cannot "feel" about each other. In this case, they can be ionized in any time,

and the ionization time of the two electrons are essentially uncorrelated. Figure 17 (b) shows that the "knee" structure disappears.

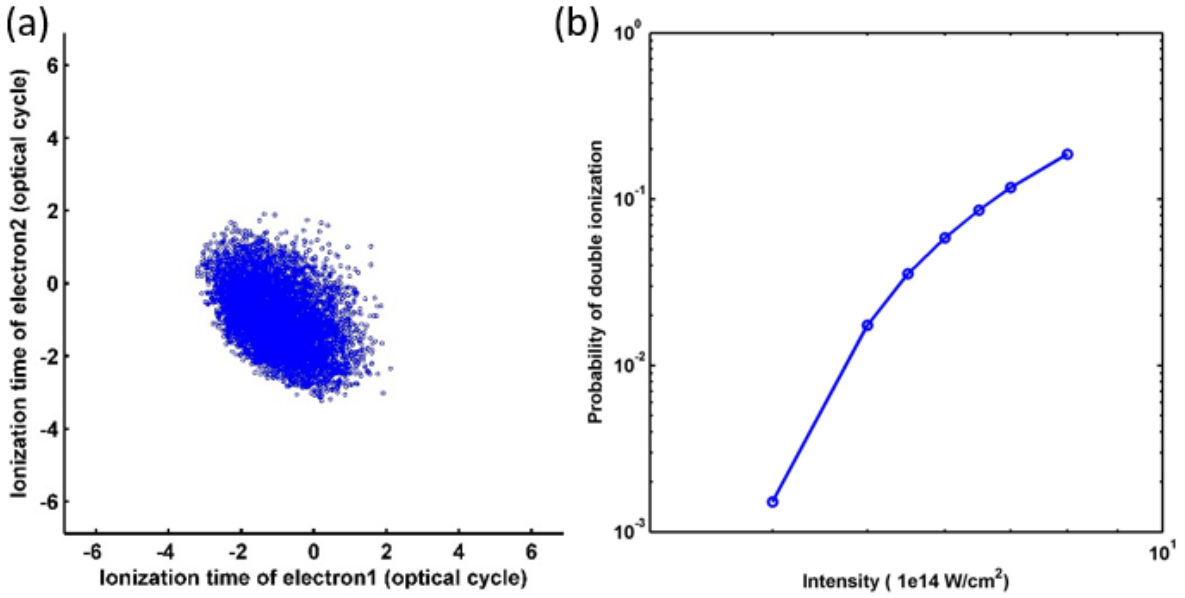

Figure 17: Correlation of ionization between electron 1 and electron 2 without the electron-electron Coulomb interaction. a) Correlation of ionization time between electron 1 and electron 2. b) The resulting double ionization.

Figure 18 shows two examples of trajectories for both the non-sequential double ionization and sequential double ionization. The red curve is the trajectory of the first electron and the blue curve is the trajectory of the second electron. r_{ionize} is defined if the electron passes through this boundary, which is considered to be ionized. In the non-sequential double ionization, the electron which is ionized first comes back to recollide the second electron. And then both of them "escape" from the ion. In the sequential double ionization, the electron that is ionized first will not came back. Later, the other electron was ionized.

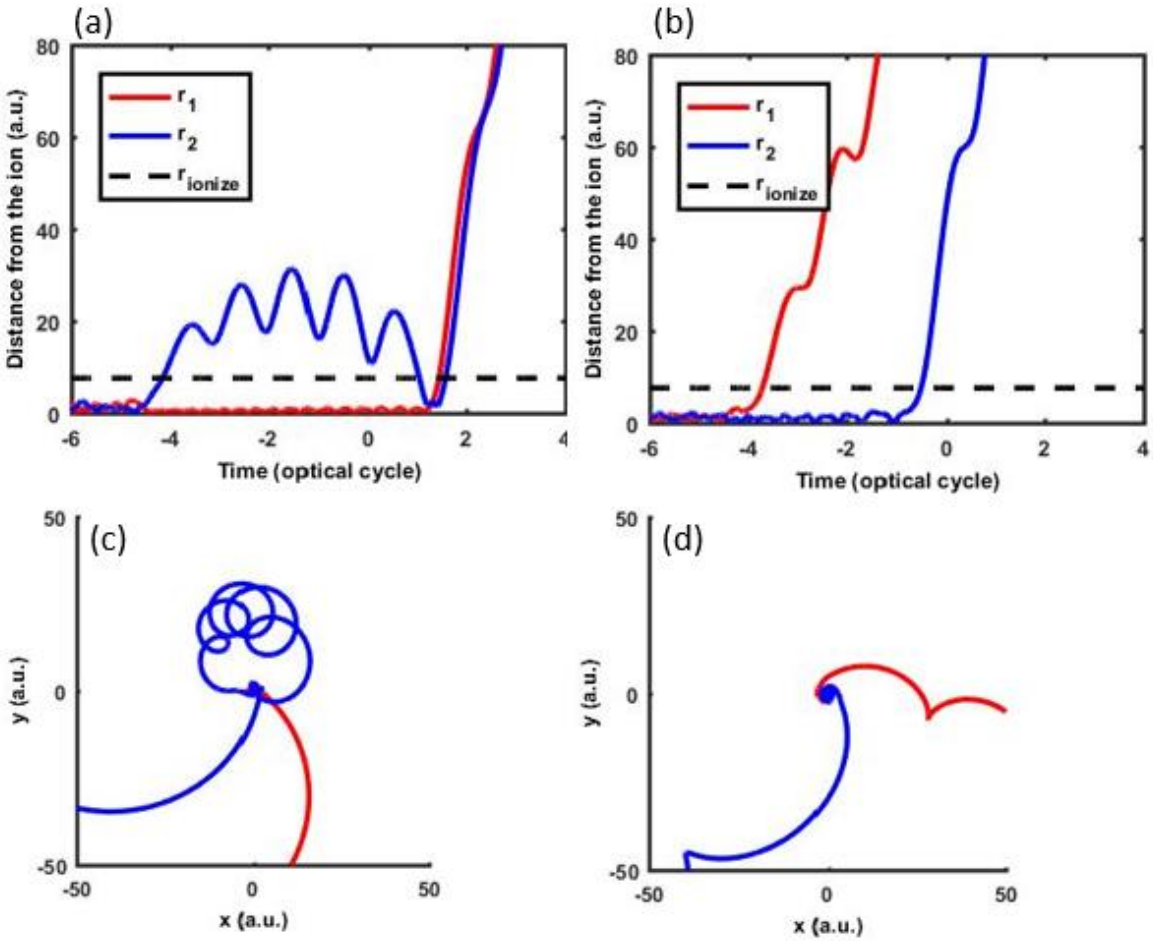

Figure 18: Trajectories of double ionization. a) Electrons trajectories of a non-sequential double ionization event respect to time. b) Electrons trajectories of a sequential double ionization event respect to time. c) Electrons trajectories of a non-sequential double ionization event in the xy plane. d) Electrons trajectories of sequential double ionization event in the xy plane. All calculations were performed on Xe atom at 400nm with the intenstiy 800TW/cm^2.

We also analyze the time difference between the outgoing electron exit the boundary and the time that it re-enter the boundary again to recollide another electron, which is the time that stays in the "continuum" before recollision. Figure 19 shows the time difference for two different laser intensities. Although the intensities are different, the time it spends in the "continuum" is about the same. The ionized electron needs a few optical cycle to come back to the ion. The reason is that the Coulomb potential between electron and ion takes some time to attract the electron back to the ion. For higher intensity, there are more non-sequential double ionization events.

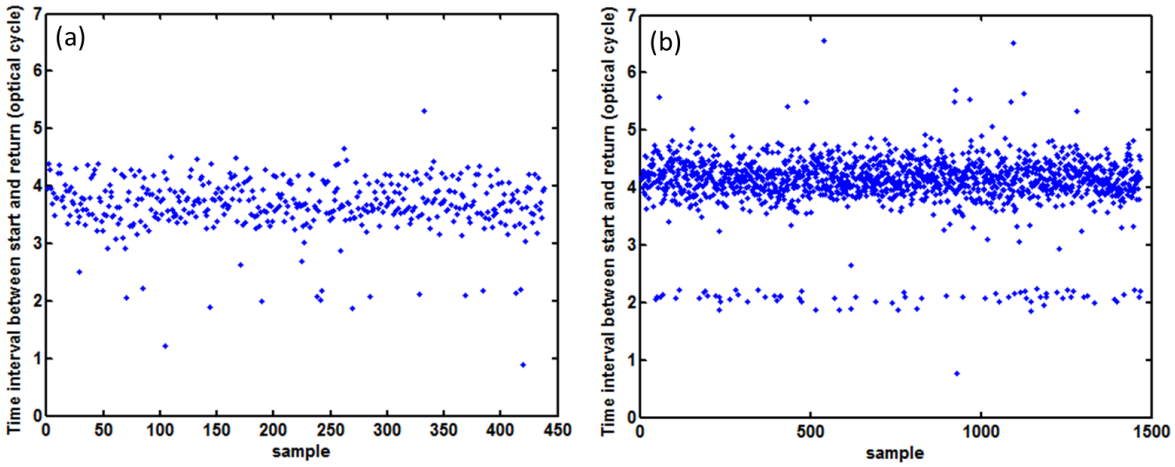

Figure 19: Time difference between the first election to pass through the boundary a) at 400 TW/cm^2; b) at 800TW/ cm^2. Both cases are from the results of Xe at 400nm.

From the analysis above, we can count the number of sequential and non-sequential ionization events from the overall ionization. We use two different methods to distinguish non-sequential double ionization and sequential double ionization, as shown in Figure 20. One way is to compare the ionization time of two electrons. As mentioned before, if the ionization time of electron 1 and electron 2 are close (<50 a.u.), we assign it to non-sequential double ionization. Otherwise, it is sequential double ionization. When the intensity is very high, sequential ionization can occur because the second electron can absorb enough energy to be ionized without the recollision. However, one drawback of this method is that it overlooks the events in which the second electron is not knocked out immediately after being collided by the returning electron, it is just excited and then ionized sometime later by the field.

Perhaps a way to make the distinction is by counting the number of times that the electron pass through the boundary, which is shown in Figure 15. If an electron passes through the boundary for at least three times, that means an electron leave the ion and then recollide and finally is ionized. Figure 20 (b) shows that the number of non-sequential double ionizations is counted by using second method is more than that by using the first method.

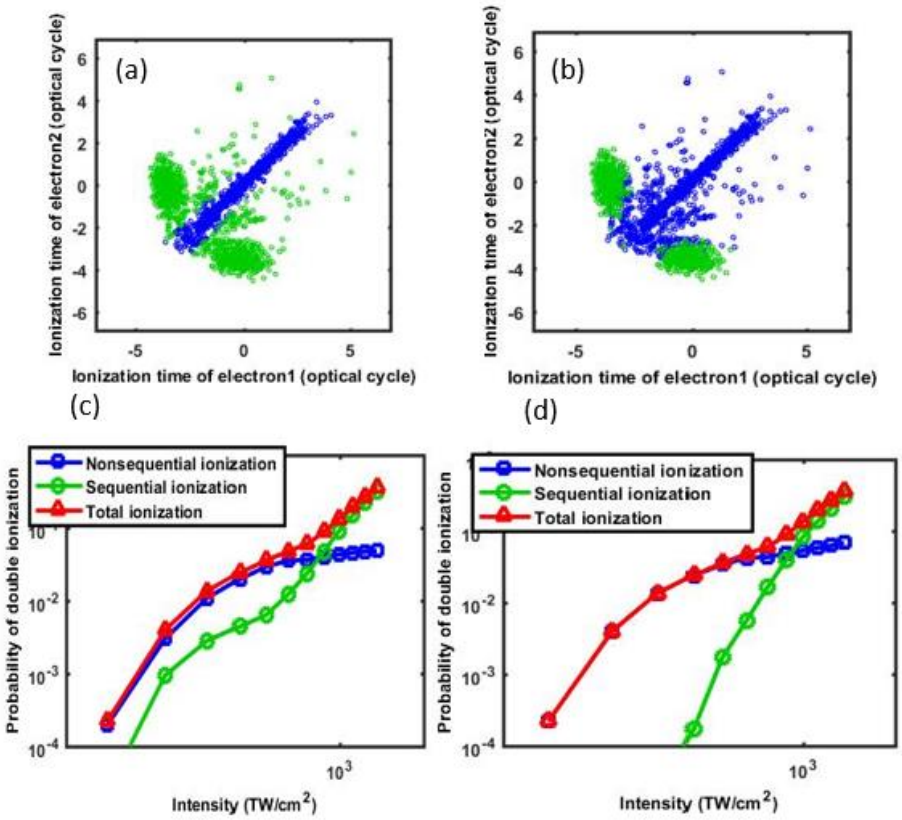

Figure 20: Analysis of double ionization by using different methods. a) The correlation of ionization time of electron 1 and electron 2 by method 1. b) The correlation of ionization time of electron 1 and electron 2 by method 2. c) The double ionization data of method 1. d) The double ionization data of method 2.

To investigate the wavelength and target dependence of the process, we look into the results of Mg at 800nm as shown in Figure 21. The results are consistence with the previous analysis of Xe. At low intensity, the domination is non-sequential double ionization. The probability of sequential double ionization increases in high intensity.

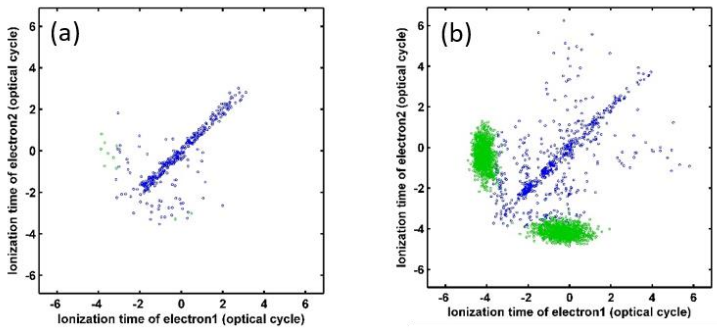

Figure 21: Correlation of ionization time between electron 1 and electron 2 of Magnesium with 800nm laser. a) The result of intensity of 120 TW/cm^2. b) The result of intensity of 250 TW/cm^2.

Furthermore, we want to explore the KE of first ionized electron when it comes back to recollide with the other electron. As show in Figure 22, the first ionized electron has KE=Up approximately as expected in circularly polarized field. Eventually, it is attracted to the ion due to the Coulomb potential of the ion. However, when it returns to the ion, it is repelled to another electron. In this case, the KE decreases. After the recollision, the first ionized electron transfers the KE to the other electron. Consequently, the other electron has enough KE that can be ionized. Therefore, in contrary to the case of LP field, the recolliding electron in CP field is mainly accelerated by the Coulomb field of the ion.

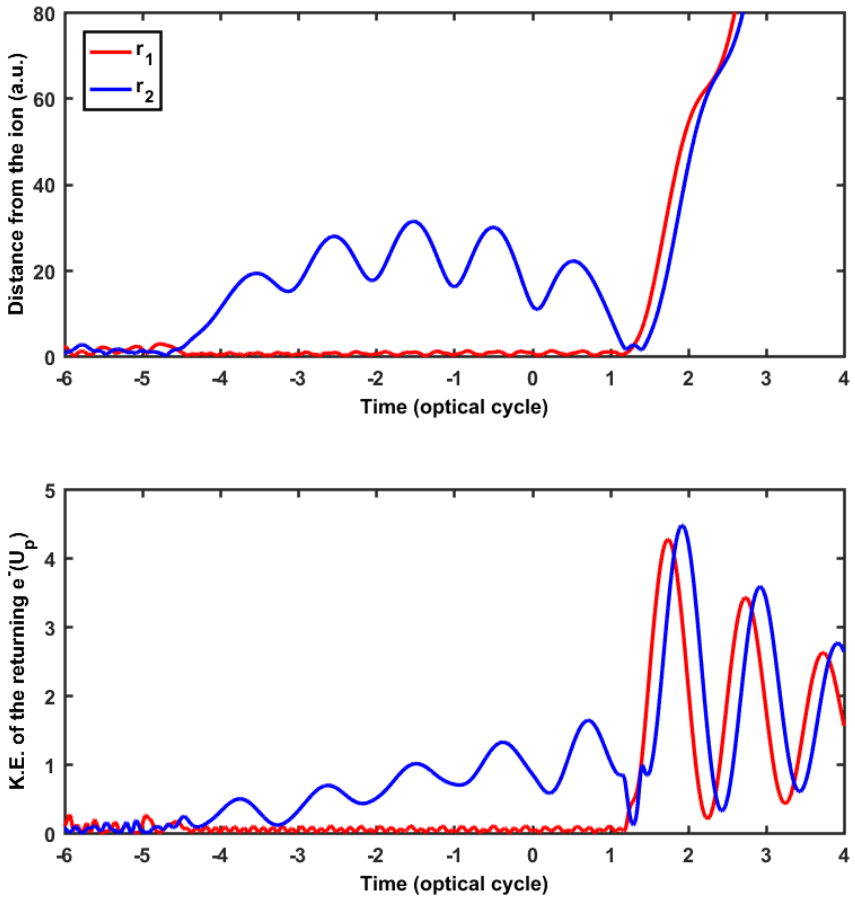

Figure 22: Non-sequential double ionization. (a) The distance between the two electrons respect to time. (b) The kinetic energy of the first ionized electron respect to time.

5. Conclusion

Non-sequential double ionization with circularly polarized fields are of interest is because it was believed that electron recollisions cannot happen in this case. However, with the influence of Coulomb potential, it can happen under certain condition. One interesting result of this study is that in circular polarization, the non-sequential double ionization is due to the Coulomb interaction rather than the laser acceleration as in the linear polarization case. According to our calculation and analysis, the phenomena of non-sequential double ionizations are related to the ionization potential I_p of atom and wavelength of laser. One key is to keep the quiver amplitude small so that the Coulomb potential of the ion can pull the electron back to it. Since the quiver amplitude, $\frac{F_0}{\omega^2}$, is proportional to the field amplitude, we need to use a low I_p atom. It is not required to have a very large field to ionize the first electron. Simultaneously, $\frac{F_0}{\omega^2}$ shows that it is more likely to have non-sequential double ionization in short wavelength. For the same atom, in low intensity, the non-sequential double ionization dominate the phenomena of double ionizations. More and more sequential double ionization occurs when the intensity becomes higher and higher.

6. References

[1] B. Walker, B. Sheehy, L. F. DiMauro, P. Agostini, K. J. Schafer, & K. C. Kulander, Phys. Rev. Lett.73, 1227 (1994).

[2] D. N. Fittinghoff, P. R. Bolton, B. Chang, & K. C. Kulander, Phys. Rev. A 49, 2174 (1994).

[3] G. D. Gillen, M. A. Walker, & L. D. VanWoerkom, Phys. Rev. A64, 043413 (1994).

[4] C. Guo & G. N. Gibson, Phys. Rev. A 63, 040701(R) (2001); C. Guo et al., ibid.58, R4271 (1998).

[5] F. Mauger, C. Chandre, & T. Uzer,Phys. Rev. Lett. 105, 083002 (2010).

[6] L. B. Fu, G. G. Xin, D. F. Ye, & J. Liu, Phys. Rev. Lett. 108, 103601 (2012).

[7] X. Wang & J. H. Eberly, Phys. Rev. Lett. 105, 083001 (2010)

[8] K. J. Schafer, B. Yang, L. DiMauro, and K. Kulander, Phys. Rev. Lett. 70, 1599 (1993).

[9] P. B. Corkum, Phys. Rev. Lett. 71, 1994 (1993).